Amorphous-to-fcc transition in $Ge_2Sb_2Te_5$ thin films: kinetics and effects of doping

S. Privitera, E. Rimini, C. Bongiorno,
CNR-IMM Stradale Primosole 50, 95121 Catania, Italy
R. Zonca
STMicroelectronics, Central R&D, Via Olivetti 2,
20041, Agrate Brianza (MI), Italy.

ABSTRACT

The amorphous-to-crystal transition has been studied through *in situ* resistance measurements in $Ge_2Sb_2Te_5$ thin films doped by ion implantation with Nitrogen or Oxygen. The dependence of the electrical resistivity and structure on the annealing temperature and time has been investigated in samples with different dopant concentrations. Enhancement of the thermal stability and increase of the mobility gap for conduction have been observed in O and N amorphous doped $Ge_2Sb_2Te_5$. Larger effects have been found in the case of Nitrogen doping. The electrical properties have been related to the structural phase change through *in situ* transmission electron microscopy analysis. The comparison between undoped and doped $Ge_2Sb_2Te_5$ shows that the introduction of oxygen or nitrogen modifies in a different way the kinetics of the amorphous-to-*fcc* transition.

Keywords: Phase transitions, Transmission electron microscopy, electrical measurements, doping

1. INTRODUCTION

GeSbTe alloys, have been recently proposed for phase change nonvolatile random access memories (PCRAM), based on the rapid phase change which occurs in chalcogenide alloys under the influence of fast electric current pulses[1]. The structural reversible phase change is the storage mechanism and the two logic states are represented by the crystalline (low resistivity) versus the amorphous phase (high resistivity). Compared to other technologies proposed to extend non volatile memories beyond the 65 nm node[2], PCRAMs present some potential advantages, such as a relatively simple structure, the possibility to be programmed to intermediate resistance values (e.g. for multi-state data storage), and a high scalability, since the energy required for phase transition decreases with cell size, allowing the scaling of the write/erase current with cell size. However, phase change recording presents also several problems. The low crystallization temperature (around 150 °C) adversely affects the stability of the amorphous phase, making PCRAMs not suitable for applications in which high temperature data retention is required. Moreover, degradation phenomena depending on the recording media composition[3] or due to its interaction with the surrounding layers[4] could reduce the cyclability. It has been shown through optical and calorimetric measurements, that nitrogen or oxygen doping may be used to improve the cyclability of phase change optical recording disks and to increase the crystallization temperature[5,6,7]. Very recently, nitrogen doped $Ge_2Sb_2Te_5$ (GST) has been also proposed for PCRAMs to enhance the cell endurance and to reduce the writing current[8]. In this paper we have investigated the effects of Nitrogen or Oxygen doping on the electrical properties of amorphous GST and on its thermal stability by measuring the resistivity during the transformation into the polycrystalline face centred cubic (*fcc*) phase. The kinetics of the amorphous-to-crystal transition have been studied by in situ transmission electron micrscopy (TEM) analysis in films doped with nitrogen and oxygen.

2. EXPERIMENTAL

Samples were prepared by depositing $Ge_2Sb_2Te_5$ (GST) films, 50 nm thick, from a single target, over oxidized Si wafers. Doping has been obtained by ion implantation of Nitrogen or Oxygen. The energy of the N and O ions was 15 keV, in order to have distributions peaked at the center of the film. Different doses were implanted, obtaining samples with peak concentrations of 1.5 at. % and 10 at.% of Nitrogen; 1.5 at.% and 6 at.% of Oxygen. Undoped samples were prepared and analyzed for comparison. The sheet resistance was measured in situ using a four-point probe configuration.

In situ transmission electron microscopy (TEM) analyses were performed by using a JEOL JEM 1010 equipped with a hot stage, which allows sample heating into the microscope. Specimens for TEM analysis were prepared by adopting an etching procedure instead of the common ion milling, in order to avoid the sample heating above the crystallization temperature during the preparation. The effects of the electron beam on the crystallization have been minimized by switching off the electron beam current during the in situ thermal treatments and by observing only fresh areas. In order to have a reliable statistical determination of the grain size and number, total areas larger than 10 μm^2 have been analyzed for each time step.

3. RESULTS

3.1. ELECTRICAL MEASUREMENTS

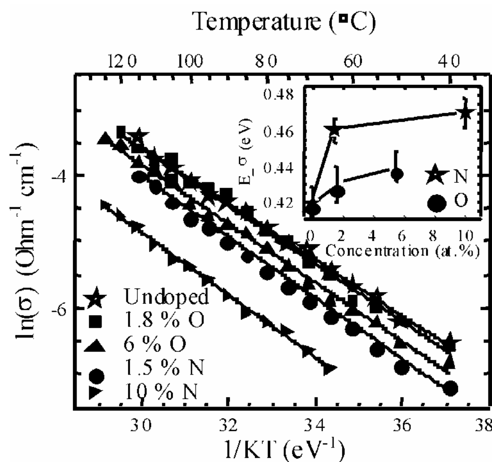

Fig. 1 Arrhenius plot of the conductivity for samples with different dopant concentration.

The conductivity of amorphous samples, in the temperature range we studied (40-120 ºC), is dominated by the band conduction through extended states, with a mobility gap whose value is about twice the activation energy for conduction E_{σ}[9]. Figure 1 shows the conductivity of amorphous samples as a function of the reciprocal temperature, measured in undoped GST (stars), and in samples with 1.5 at.% of O (squares), 6 at.% of O (triangles), 1.5 at.% of N (circles) and 10 at.% of N (flags). As the dopant concentration increases, the conductivity decreases and the activation energy for conduction, E_{σ}, slightly increases, as shown in the insert of Fig. 1, where the measured activation energies have been plotted as a function of dopant concentration. Stars and squares in the insert refer to Nitrogen and Oxygen doped samples, respectively. Therefore, the mobility gap in the amorphous GST monotonically increases as the dopant concentration increases. Larger variations have been obtained in the case of Nitrogen: by doping GST with 10 at. % of N, the conductivity decreases of one order of magnitude and E_{σ} increases from 0.42 ± 0.01 eV, measured in undoped samples, up to 0.47 ± 0.01 eV.
At temperatures higher than 120 ºC, after an incubation period which depends on the annealing temperature[10,11], the resistivity sharply decreases as a function of time, indicating the conversion of the material into the polycrystalline *fcc* phase. Figure 2 shows the behavior of the resistivity as a function of the annealing time for undoped samples (a) and with 6 at.% of O (b), under annealing at temperatures in the range 130-190 ºC. Samples doped with 6 at. % of O exhibit the same trend of undoped samples, but are characterized by slightly longer incubation times at low temperature and by higher transition rates. The variation of the resistivity upon transition in O doped GST is comparable to that measured in undoped material (equal to about three orders of magnitude) or higher.

Figure 3 (a) and (b) shows the resistivity measured at different temperatures as a function of time for samples with 1.5 at.% and 10 at.% of N, respectively. The addition of Nitrogen produces a large increase of the incubation time. In the case of 10 at.% of N, the transition rate is much lower and the resistivity change from the amorphous to the *fcc* phase is reduced to about two orders of magnitude.
From figures 2 and 3 it is possible to evaluate the activation energy for the crystallization, which depends on both the nucleation and growth processes involved in the transformation. Figure 4 shows the Arrhenius plot of the characteristic times, for different dopant species and concentrations. Characteristic times have been evaluated as the time at which the first derivative of the resistivity versus time

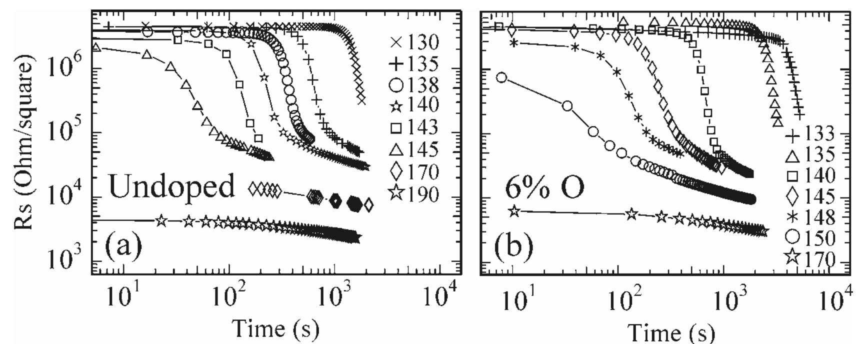

Fig. 2 Resistivity as a function of annealing time for different temperatures for undoped (a), and O 6 at.% doped samples (b).

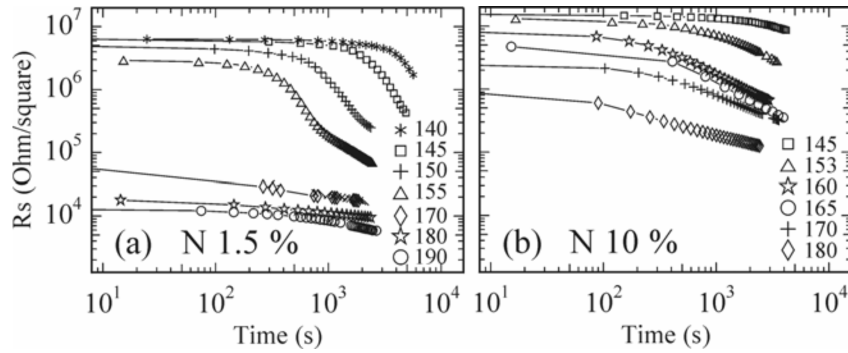

Fig. 3 Resistivity as a function of annealing time for different temperatures for samples doped with 1.5 at. % of N (a), and 10 at.% of N (b).

exhibits a minimum. In the case of 10 at.% of N, it was not possible to evaluate the activation energy because of the different shape of the resistivity as a function of time, whose derivative does not exhibit a minimum. Characteristic times of undoped samples are lower than those measured for oxygen or nitrogen doped GST. The activation energy for the transformation is almost the same, and equal to about 3 eV, for undoped chalcogenide and for samples with 1.5 at.% of O or 1.5 at.% of N. In GST doped with 6 at.% of O the activation energy increases up to 3.6 eV.

The differences between the various samples on the stability of the amorphous phase can be summarized by plotting the resistivity measured after isochronal anneals, as a function of temperature. Figure 5 shows the resistivity vs temperature, as measured after 12 minutes anneal. Triangles, circles, squares and stars refer to undoped, 1.5 at.% of N, 10 at.% of N and 6 at.% of O, respectively. In samples doped with 10 at.% of N the crystallization temperature increases of about 45 °C .

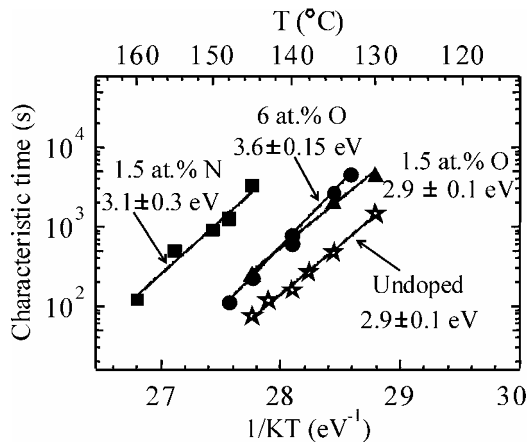

Fig. 4 Arrhenius plot of characteristic times, obtained for different samples

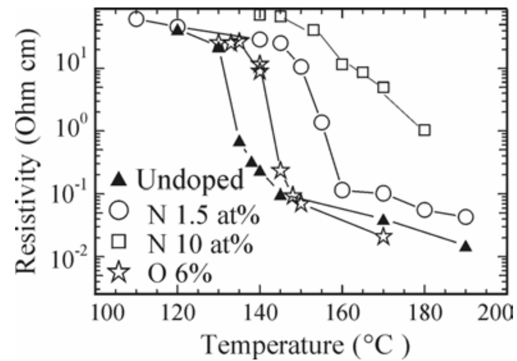

Fig.5 Resistivity versus temperature, as measured after 12 min anneals.

3.2. IN SITU TRANSMISSION ELECTRON MICROSCOPY

3.2.1. Undoped Samples

The results obtained from the electrical measurements can be related to the kinetics of the nucleation and growth phenomena through in situ transmission electron microscopy analyses. Figure 6 (a), (b) and (c) shows typical TEM plan view images acquired in bright field for undoped samples after annealing at 137 °C for 55 min, 75 min and 105 min, respectively. Crystalline grains embedded in the amorphous matrix appear as dark or bright regions.

The addition of 1.5 at.% of N produces strong variations in the kinetics of the transformation. Figure 7 (a), (b) and (c) shows plan view images obtained in samples with 1.5 at. % of N after annealing at 140 °C for 150 min, 250 min and 290 min, respectively. In agreement with previously reported results, obtained by doping the GST film during the

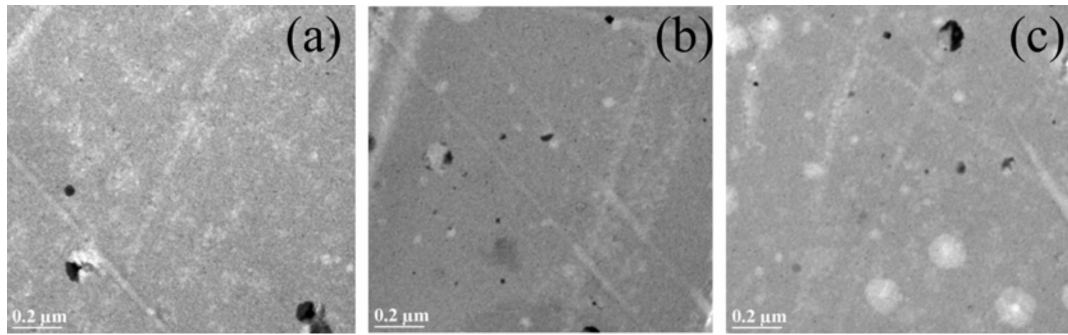

Fig. 6 Plan view images in bright field of an undoped sample annealed in situ at 137 ºC for 55 min (a), 75 min (b) and 105 min

deposition[5,7], the addition of nitrogen by ion implantation, strongly increases the incubation time and reduces the grain size. This appears mainly due to a reduction of the growth velocity. In situ TEM analyses in cross section, show that in nitrogen doped samples, the nucleation occurs at the interface with the SiO_2 substrate layer, as already observed for undoped GST[12] or GST over Silicon[13], even if, in this case, the GST/SiO_2 interface could be modified by the

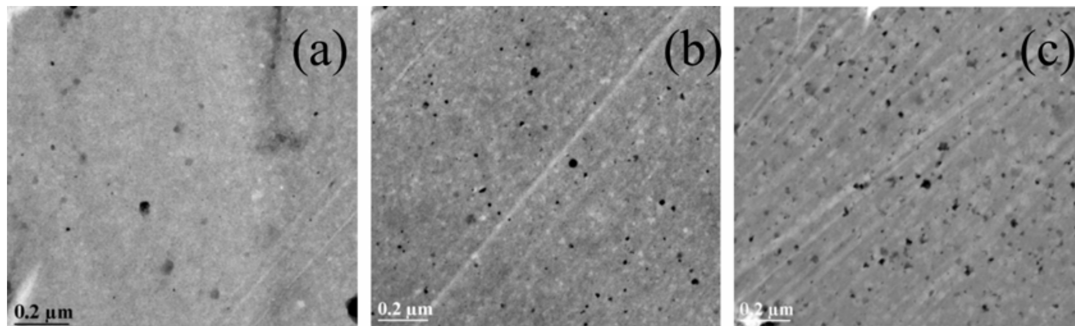

Fig. 7 Plan view images in bright field of a sample doped with 1.5 at. % of N, annealed in situ at 140 ºC for 150 min (a), 250 min (b) and 290 min (c).

implantation. As an example, Fig. 8 (a), (b) and (c) shows the earl stage of the crystallization in GST doped with 1.5 at.% of N, after annealing at 140 °C for 10 min, 15 min and 50 min, respectively. After 10 min at 150 ºC the chalcogenide film is still amorphous, but after 15 min some crystalline grains appear at the interface with the substrate layer. To evidence the grain formation, fig. 8 (b) has been acquired in dark field configuration. If we increase the thermal treatment up to 50 min, the grains nucleated at the interface with the SiO_2 form a continuous layer, while the remaining film is amorphous, except for a few grains formed at the interface with the epox.

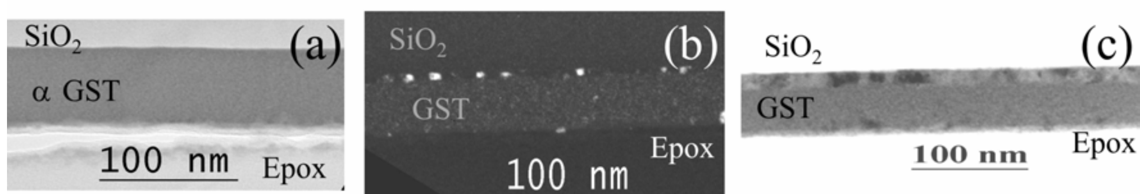

Fig. 8 TEM images in cross section of a sample doped with 1.5 at. % of N, annealed in situ at 150 ºC for 10 min (a), 15 min (b) and 50 min (c).

The effects of Oxygen doping are quite different from those of Nitrogen, as shown from figure 9 (a), (b) and (c), which reports TEM images in bright field of samples doped with O 6 at.%, after annealing at 137 ºC for 50 min, 60 min and 70 min, respectively. The comparison with the undoped sample annealed at the same temperature (fig. 6) shows that the presence of oxygen increases the average grain size. Moreover, the transition rate in O doped samples becomes higher

compared to undoped samples, as the annealing temperature increases. These results are in agreement with the resistance measurements, which show higher activation energy for samples with 6 at.% of O.

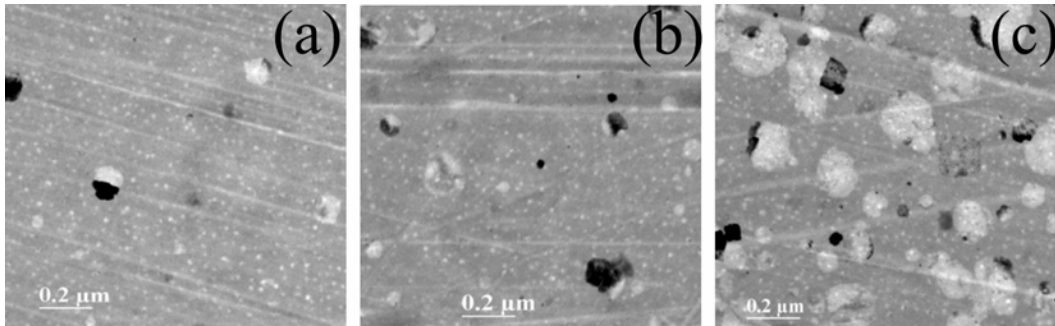

Fig. 9 TEM images of a sample doped with 6 at. % of O annealed in situ at 137 ºC for 50 min (a), 60 min (b) and 70 min (c).

4. DISCUSSION

The increase of the crystallization temperature in Oxygen[6] and Nitrogen[5,7] doped GST, as well as the reduction of the grain size in Nitrogen doped samples, have been already reported in literature. Two models have been proposed to account for increase crystallization temperature and for the optical properties of doped GST[6,7] : one involving the strain field, and the other the transition of the chemical bonding state from the metallic mode to the dielectric mode. For the first model, since nitrogen and oxygen have an atomic size quite small compared to that of Ge, Sb and Te, they cannot substitute these atoms, filling the vacancies which are present in the structure (20 %). N or O will be therefore located at the tetrahedral interstitial sites distorting the unit cell and resulting in a strain field. Since nitrogen has a larger atomic radius (0.065 nm), compared to oxygen (0.06 nm), it is expected a larger amount of strain in the structure, to accommodate nitrogen atoms. Therefore a strain effect could account for the higher crystallization temperature and the larger mobility gap, observed in the case of Nitrogen doping. However, this explanation seems to not agree very well with the higher growth velocity observed in oxygen doped samples. Moreover, as the amount of Nitrogen or Oxygen into the GST increases, some atoms are expected to precipitate into nitrides or oxides. Indeed, the segregation of these compounds at the grain boundaries has been proposed to explain the increase of the cyclability and the reduction of the grain size, observed in nitrogen doped GST[5]. On the basis of results reported in literature[5], this segregation should occur for nitrogen concentrations above 1.5 at. %. We cannot therefore exclude, in the samples doped by ion implantation with 10 at.% of N, the formation of very thin nitrides layers at the grain boundaries, which are probably responsible for the increased resistivity of the crystalline phase and the smoothing of the shape of the resistivity versus time, as shown in Fig. 3(b). No nitride layers have been revealed at the grain boundaries in samples with 1.5 at.% of N, even if the measured average grain size is much lower than in undoped samples.
According to the second model proposed in literature[6,7], since oxides and nitrides are more covalent than GST, some of the chemical bonds are expected to change towards more covalent bonds. The difference between the electronegativity of Nitrogen (3.04)[14] and that of Ge, Sb and Te (around 2)[14] is lower, compared to that of Oxygen (3.44)[14]. Moreover, Nitrogen can form three bonds while Oxygen is bivalent. Therefore Nitrogen could be more effective in forming covalent bonds which may saturate defects in the amorphous material, increasing the mobility gap and reducing the conductivity. The presence of more covalent bonds may also reduce the atomic diffusivity, leading to an increase of the crystallization temperature and a lower grain size.

5. CONCLUSIONS

The effects of Nitrogen or oxygen doping of $Ge_2Sb_2Te_5$ by ion implantation has been studied through *in situ* electrical measurements and transmission electron microscopy. An increase of the incubation time of about one order of

magnitude and a strong reduction of the growth velocity have been observed in samples with 1.5 at.% of N, while doping with 6 at.% of O produces small effects on the crystallization temperature but increases of about 0.6 eV the activation energy for the transformation and produces larger grain sizes. In addition, a monotonic increase of the mobility gap in amorphous films has been observed with increasing dopant concentration. The results have been explained by considering both the effect of strain fields and a more covalent bonding.

REFERENCES

1. S. Lai and T. Lowrey, Tech. Dig.- Int. Electron Devices Meet. **2001**, 36.5.1 (2001)
2. ITRS03, *International Roadmap for Semiconductors* (Clarendon, updated 2003 Edition, 2003).
3. M. Chen, K. A. Rubin, V. Marello, U. G. Gerber, and V. B. Jipson, Appl. Phys. Lett. **46**, 734 (1985).
4. N. Yamada, M. Otoba, K. Kawahara, N. Miyagawa, H. Ohta, and N. Akahira, Jpn. J. Appl. Phys. **37**, 2104 (1998).
5. R. Kojima, S. Okabayashi, T. Kashihara, K. Horai, T. Matsunaga, E. Ohno, N. Yamada, and T. Ohta, Jpn. J. Appl. Phys. **37**, 2098 (1998).
6. T. H. Jeong, H. Seo, K. L. Lee, S. M. Choi, S. J. Kim, and S. Y. Kim, Jpn. J. Appl. Phys.**40**, 1609 (2001).
7. T. H. Jeong, M. R. Kim, H. Seo, J. W. Park, , and C. Yeon, Jpn. J. Appl. Phys. **39**, 2775(2000).
8. H. Horii, J. H. Yi, Y. H. Ha, I. G. Baek, S. O. Park, Y. N. Hwang, S. H. Lee, Y. T. Kim, K. H. Lee, U.-I. Chung, et al., 2003 Symp. on VLSI Techn. Dig. of Tech. Papers **12B-5**, 177 (2003).
9. N. F. Mott and E. A. Davis, *Electronic processes in Non-Crystalline Materials* (Clarendon, Oxford, (1979)).
10. I. Friedrich, V. Weidenhof, W. Njorge, P. Franz, and M. Wuttig, J. Appl.Phys. **87**, 4130 (2000).
11. S. Privitera, E. Rimini, C. Bongiorno, R. Zonca, A. Pirovano, and R. Bez, J. Appl. Phys. **94**,4409 (2003).
12. S. Privitera, C. Bongiorno, E. Rimini and R. Zonca, Appl. Phys. Lett. **84**, 4448 (2004)
13. T. H. Jeong, M. R. Kim, H. Seo, S. J. Kim and S. Y. Kim, J. Appl.Phys. **86**, 774 (1999).
14. CRC Handbook of Chemistry and Physics (CRC Press, 2003-2004).